J Physiol 596.15 (2018) pp 3171–3185

The Journal of Physiology

KLF2 mediates enhanced chemoreflex sensitivity, disordered breathing and autonomic dysregulation in heart failure

Noah J. Marcus[1,2], Rodrigo Del Rio[1,3], Yanfeng Ding[1,4] and Harold D. Schultz[1]

[1] *Department of Cellular and Integrative Physiology, University of Nebraska Medical Center, Omaha, NE, USA*
[2] *Department of Physiology and Pharmacology, Des Moines University, Des Moines, IA, USA*
[3] *Laboratory of Cardiorespiratory Control, Universidad Autónoma de Chile, Santiago, Chile*
[4] *University of North Texas Health Sciences Center, Fort Worth, TX, USA*

Key points

- Enhanced carotid body chemoreflex activity contributes to development of disordered breathing patterns, autonomic dysregulation and increases in incidence of arrhythmia in animal models of reduced ejection fraction heart failure.
- Chronic reductions in carotid artery blood flow are associated with increased carotid body chemoreceptor activity.
- Krüppel-like Factor 2 (KLF2) is a shear stress-sensitive transcription factor that regulates the expression of enzymes which have previously been shown to play a role in increased chemoreflex sensitivity.
- We investigated the impact of restoring carotid body KLF2 expression on chemoreflex control of ventilation, sympathetic nerve activity, cardiac sympatho-vagal balance and arrhythmia incidence in an animal model of heart failure.
- The results indicate that restoring carotid body KLF2 in chronic heart failure reduces sympathetic nerve activity and arrhythmia incidence, and improves cardiac sympatho-vagal balance and breathing stability. Therapeutic approaches that increase KLF2 in the carotid bodies may be efficacious in the treatment of respiratory and autonomic dysfunction in heart failure.

Abstract Oscillatory breathing and increased sympathetic nerve activity (SNA) are associated with increased arrhythmia incidence and contribute to mortality in chronic heart failure (CHF). Increased carotid body chemoreflex (CBC) sensitivity plays a role in this process and can be precipitated by chronic blood flow reduction. We hypothesized that downregulation of a shear stress-sensitive transcription factor, Krüppel-like Factor 2 (KLF2), mediates increased CBC sensitivity in CHF and contributes to associated autonomic, respiratory and cardiac sequelae. Ventilation (Ve), renal SNA (RSNA) and ECG were measured at rest and during CBC activation in sham and CHF rabbits. Oscillatory breathing was quantified as the apnoea–hypopnoea index (AHI) and respiratory rate variability index (RRVI). AHI (control 6 ± 1/h, CHF 25 ± 1/h), RRVI (control 9 ± 3/h, CHF 29 ± 3/h), RSNA (control 22 ± 2% max, CHF 43 ± 5% max) and arrhythmia incidence (control 50 ± 10/h, CHF 300 ± 100/h) were increased in CHF at rest (F_{IO_2} 21%), as were CBC responses (Ve, RSNA) to 10% F_{IO_2} (all $P < 0.05$ *vs.* control). *In vivo* adenoviral transfection of KLF2 to the carotid bodies in CHF rabbits restored KLF2 expression, and reduced AHI (7 ± 2/h), RSNA (18 ± 2% max) and arrhythmia incidence (46 ± 13/h) as well as CBC responses to hypoxia (all $P < 0.05$ *vs.* CHF empty virus). Conversely, lentiviral KLF2 siRNA in the carotid body decreased KLF2 expression, increased chemoreflex sensitivity, and increased AHI (6 ± 2/h *vs.* 14 ± 3/h), RRVI (5 ± 3/h *vs.* 20 ± 3/h) and RSNA (24 ± 4% max *vs.* 34 ± 5% max) relative to scrambled-siRNA rabbits. In conclusion, down-regulation of KLF2 in the carotid

DOI: 10.1113/JP273805

body increases CBC sensitivity, oscillatory breathing, RSNA and arrhythmia incidence during CHF.

(Received 21 November 2016; accepted after revision 31 August 2017; first published online 6 September 2017)
Corresponding author N. J. Marcus: Department of Physiology and Pharmacology, Des Moines University, Des Moines, IA 50312-4198, USA. Email: noah.marcus@dmu.edu

Abbreviations ACE1, angiotensin-converting enzyme 1; AHI, apnoea–hypopnoea index; CHF, chronic heart failure; CB, carotid body; CBC, carotid body chemoreflex/chemoreceptor; eNOS, endothelial nitric oxide synthase; GFP, green fluorescent protein; HRV, heart rate variability; HF, high frequency of heart rate variability; KLF2, Krüppel-like Factor 2; LF, low frequency of heart rate variability; RRVI, respiratory rate variability index; RSNA, renal sympathetic nerve activity; SDNN, standard deviation of the normal to normal R–R interval; SNA, sympathetic nerve activity; V_E, minute ventilation; V_t, tidal volume.

Introduction

Autonomic dysregulation and sleep-disordered breathing are positively correlated with increased arrhythmia incidence in patients with chronic heart failure (CHF) (Giannoni *et al.* 2008). Multiple lines of evidence suggest that autonomic dysregulation in CHF is positively correlated with oscillatory breathing (Naughton *et al.* 1995, van de Borne *et al.* 1998), and alterations in cardiovascular reflexes and central neural control of sympathetic nerve activity (SNA) (Zucker *et al.* 2004). Recent work from our laboratory suggests strongly that an enhanced carotid body chemoreflex (CBC) plays a central role in the development of autonomic imbalance and disordered breathing patterns in CHF (Del Rio *et al.* 2013; Haack *et al.* 2014; Marcus *et al.* 2014). The significance of these observations is underlined by the finding that mortality risk is higher in CHF patients with high chemosensitivity relative to comparable CHF patients with normal chemosensitivity (Ponikowski *et al.* 2001; Giannoni *et al.* 2008).

Previous work has shown that the mechanisms underlying changes in CBC function in CHF include reductions in nitric oxide bioavailability and cytoplasmic/mitochondrial superoxide dismutase as well as increases in angiotensin II metabolism and oxidative stress (Li *et al.* 2005, 2006; Ding *et al.* 2009, 2010). We have recently demonstrated that blood flow to the carotid body (CB) is chronically reduced in experimental CHF, that these chronic reductions alone are sufficient to elicit alterations in nitric oxide and angiotensin metabolism, and that chronic reductions in CB blood flow enhance chemoreflex function to the same extent as observed in CHF (Ding *et al.* 2010).

Krüppel-like Factor 2 (KLF2) is a mechano-sensitive transcription factor that is induced by shear stress in the vasculature and controls transcription of target genes associated with nitric oxide bioavailability, angiotensin metabolism, antioxidant defences and inflammation (Dekker *et al.* 2005). For these reasons, we postulated that chronic reductions in blood flow in CHF might affect CBC activity via reductions in CB KLF2 expression. Indeed, our previous work confirms that CB KLF2 expression is reduced in coronary artery ligation-induced CHF, and that this is associated with increased CBC sensitivity, oscillatory breathing patterns and arrhythmia incidence (Haack *et al.* 2014). We also found that treatment with Simvastatin had a salutary effect on these changes and was associated with increased CB KLF2 expression. These studies provide supportive evidence for our hypothesis but they do not demonstrate causality between reductions in CB KLF2 and enhanced CBC function in CHF. With this in mind, we sought to clearly delineate the role of CB KLF2 in the enhanced CBC function observed in CHF. To address this question, we used viral vectors to selectively alter CB KLF2 expression in CHF and healthy rabbits.

In the present study, we hypothesized that CB KLF2 expression would be reduced with the development of CHF in rabbits. Furthermore, we hypothesized that selective restoration of KLF2 in CB tissue would normalize CBC function, resulting in concomitant reductions in SNA, disordered breathing and arrhythmia incidence. We measured renal sympathetic nerve activity (RSNA) and ventilation at rest and in response to hypoxia to characterize the sensitivity of the CBC and determine the effect of CB KLF2 restoration on CBC function and its contribution to resting RSNA, oscillatory breathing patterns and arrhythmia incidence in CHF. Furthermore, to fully unveil the role played by KLF2 in the development of heightened CBC activity we performed an additional set of studies using a different vector to selectively knock-down CB KLF2. *In vivo* delivery of KLF2 siRNA to the CB was performed in otherwise healthy rabbits and we examined the effect on CBC function, autonomic function and resting breathing.

Methods

Ethical approval and statement of compliance

The experimental protocols were approved by the University of Nebraska Medical Center Institutional Animal Care and Use Committee and were carried out in accordance with the National Institutes of Health (NIH

Publication No. 85-23, revised 1996) and the American Physiological Society's Guide for the Care and Use of Laboratory Animals. The authors understand the ethical principles under which the *Journal of Physiology* operates and wish to declare that our work complies with the animal ethics checklist outlined by Grundy (2015).

Experimental groups

Thirty-eight adult male New Zealand White rabbits weighing 3.5–4.0 kg were obtained from Charles River Laboratories (Wilmington, MA, USA). All rabbits were housed in individual cages under controlled temperature and humidity and a 12:12 h dark–light cycle, and fed standard rabbit chow with water available *ad libitum*. Rabbits were randomly assigned to one of the following experimental groups: (1) sham: chest surgery without pacing, $n = 8$; (2) CHF-empty: chest surgery, pacing protocol and underwent virus surgery in which empty green fluorescent protein (GFP)-tagged adenovirus was delivered to CB, $n = 8$; (3) CHF-KLF2: chest surgery, pacing protocol and underwent virus surgery in which KLF2 GFP-tagged adenovirus was delivered to CB, $n = 8$; (4) scrambled siRNA: chest surgery without pacing, and underwent virus surgery in which scrambled siRNA GFP-tagged lentivirus was delivered to CB, $n = 6$; (5) KLF2-siRNA: chest surgery without pacing, and underwent virus surgery in which KLF2 siRNA GFP-tagged lentivirus was delivered to CB, $n = 8$. All groups followed similar timelines as described below and in Fig. 1.

Anaesthetic protocol and monitoring procedures

For all surgeries, anaesthesia was induced with a cocktail of 5.8 mg kg^{-1} xylazine, 35 mg kg^{-1} ketamine and 0.01 mg kg^{-1} atropine given intramuscularly. Rabbits were subsequently intubated and connected to a small animal anaesthesia respiration unit using 2.0–5.0% inhalation isoflurane with oxygen for the duration of the surgery. Prior to placement of sterile drapes the palpebral reflex was checked and the lack of a gag reflex was confirmed with placement of the endotracheal tube. Respiration was checked to determine that the animal was not breathing against the respirator, coughing or chewing the endotracheal tube. During surgical procedures, blood pressure, heart rate and ventilator compliance were monitored as indicators of adequate anaesthetic depth.

Surgical procedures for induction of CHF

A pressure telemetry unit was implanted into a branch of the femoral artery and advanced into the iliac artery or into the abdominal aorta. A left thoracotomy was performed to implant a pin electrode on the base of the left ventricle for pacing. The leads of pacing electrodes were tunnelled subcutaneously and fixed on the back. Post-operative analgesia was provided initially via 0.02 mg kg^{-1} intravenous buprenorphine administered immediately following surgery. Subsequent analgesia was provided via a fentanyl patch (25 μg h^{-1}, transdermal) for 72 h after surgery. If determined necessary by staff veterinarian(s), additional analgesia was provided by a subcutaneous injection of carprofen (4 mg kg^{-1}, daily as needed). An antibiotic regimen consisting of 5 mg kg^{-1} baytril was administered subcutaneously daily for 5 days post-operatively. Experimental protocols began 10 days after surgery when the rabbits had fully recovered.

Induction of CHF

CHF was induced by left ventricular pacing and monitored by weekly ECGs as previously described (Sun *et al.*

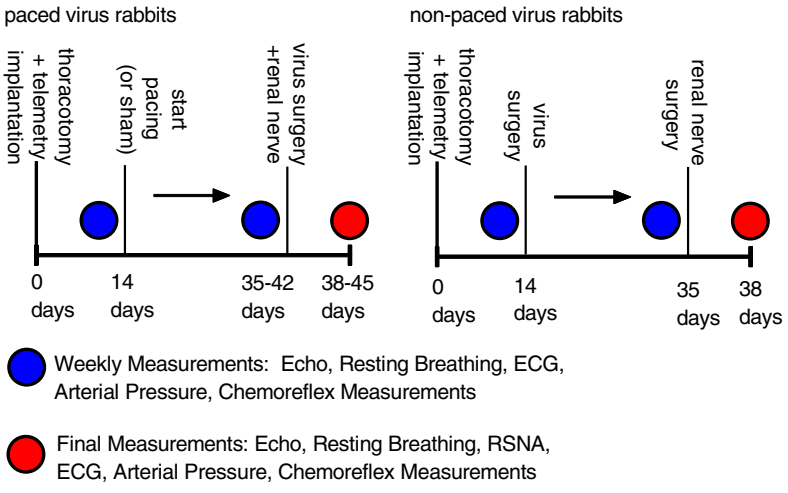

Figure 1. Experimental timelines in paced and non-paced rabbits
Left, time course of surgeries and experimental measurements in paced or sham rabbits that underwent virus surgery for delivery of adenoviral KLF2 or adenoviral empty. *Right*, time course of surgeries and experimental measurements in non-paced rabbits that underwent virus surgery for delivery of lentiviral KLF2 siRNA or lentiviral scrambled siRNA.

1999*a*, *b*; Ding *et al.* 2011; Marcus *et al.* 2014). Rapid ventricular pacing was initiated at a rate of 340 bpm, which was held for 7 days, and the rate was then gradually increased to 380 bpm, with an increment of 20 bpm each week. All rabbits were checked daily to ensure chronic pacing. The progression of CHF was monitored by weekly ECGs (Siemens/Acuson Sequoia 512C with a 4 MHz probe, Siemens Medical Solutions USA, Inc., Malvern, PA, USA) prior to virus surgery, and at 3 days after virus surgery, with the pacemaker turned off for at least 30 min before the recordings were started. Rabbits were paced continually for 3–4 weeks until >35% reduction in ejection fraction was achieved.

Chronic cardiac pacing to produce heart failure has been used extensively and is considered a reliable disease model for replication and study of the mechanical, structural and neuro-humoral alterations associated with dilatated cardiomyopathy in humans (Houser *et al.* 2012). Our pacing protocol results in decreases in ejection fraction, cardiac contractility, and increases in cardiac volume and central venous pressure, in addition to increases in renal SNA (Sun *et al.* 1999*b*).

Surgical procedures for viral transfection of CBs and implantation of renal nerve electrodes

Delivery of viral vectors to the carotid sinus was performed as previously described (Li *et al.* 2005; Ding *et al.* 2009, 2010). Only the timing of virus delivery and renal nerve implantation differed between paced and un-paced experimental groups. In paced rabbits (CHF-empty and CHF-KLF2), viral transfection and implantation of renal nerve electrodes took place after 3–4 weeks of pacing. In un-paced rabbits (scrambled siRNA and KLF2 siRNA) viral transfection took place 3 weeks prior to implantation of renal nerve electrodes. We chose to use a lentiviral vector for the siRNA experiments because the stable expression allowed us to study these rabbits along a timeline similar to paced rabbits.

In all groups, anaesthesia was induced and maintained as described in the 'Anaesthetic protocol and monitoring procedures'. Using sterile techniques, the carotid sinus regions were exposed and the CB was visually identified. The sinus region was temporarily vascularly isolated (including the common carotid artery, internal carotid artery and external carotid artery), and the tip of a PE-10 catheter was positioned in the external maxillary artery and advanced near the origin of the CB artery. After the arteries were occluded with snares, 200 μl of a virus solution (described below) was slowly injected via the catheter and allowed to incubate for 20 min, after which the solution was withdrawn and the snares around the vessels were removed. The procedure was repeated on the contralateral CB, after which the incision was closed.

The viruses used in the surgeries on paced rabbits were as follows: 1 μl of 3×10^{10} pfu ml^{-1} Adenoviral Empty-GFP (Ad-GFP, no. V1000, Welgen Inc., Worcester, MA, USA) or Adenoviral KLF2-GFP (Ad-KLF2, S3000, Welgen Inc.). The viruses used in the surgeries on un-paced rabbits were as follows: 6 μl of 10^7 IU ml^{-1} pilenti-scrambled siRNA-GFP (scrambled siRNA Lentivirus, Applied Biological Materials Inc., Richmond, BC, USA), or 6 μl of 10^7 IU ml^{-1} pilenti-KLF2 siRNA-GFP [KLF2 siRNA/shRNA/RNAi Lentivirus (Human) pooled, Applied Biological Materials Inc.]. All virus solutions were dissolved in 300 μl 0.9% sterile sodium chloride.

In all groups a pair of electrodes was implanted on the left renal sympathetic nerves during the same surgical procedure as described previously (Li *et al.* 2005, 2006; Ding *et al.* 2009). Using sterile techniques, an incision was made along the costal margin on the left side. Muscles were retracted and the kidney was approached in the retroperitoneal space. The renal artery and nerve were identified. Using glass hooks, the renal nerve was gently separated from the artery and a pair of Teflon-coated silver wire electrodes were secured to the nerve using a fast-setting silicone gel (Wacker Sil-Gel). A ground wire was sutured to a nearby muscle before the incision was closed. The electrode wires were tunnelled beneath the skin to exit on the upper back.

Post-operative analgesia was provided initially via 0.02 mg kg^{-1} buprenorphine administered intravenously immediately after surgery. Subsequent analgesia was provided by subcutaneous injection of carprofen (4 mg kg^{-1}) with frequency as needed determined by a staff veterinarian (typically, daily for 3 days following surgery). In addition, all rabbits were placed on an antibiotic regimen consisting of 5 mg kg^{-1} baytril administered subcutaneously for 5 days. CHF rabbits recovered for 24 h after surgery before cardiac pacing resumed in the CHF-empty and CHF-KLF2 groups. No experiments were performed until 3 days after surgery.

Evaluation of resting variables

All baseline and experimental measurements were obtained from paced rabbits with the pacemaker turned off for at least 30 min prior to the beginning of experiments. Rabbits were placed in a Plexiglas chamber (volume 11 litres) with exit ports for ECG wires and renal nerve electrodes, and the chamber was sealed, except for an inlet and outlet port that allowed a continuous flow of air through the chamber. Measurements of resting arterial blood pressure, ECG, ventilation and RSNA (when available) were recorded over 2 h. Arterial blood pressure was measured via a radio-telemetry transmitter (Data Science International, St Paul, MN, USA).

Chemoreflex evaluation with RSNA and minute ventilation (V_E)

To determine changes in CBC sensitivity with the development of CHF and to identify the role of KLF2, reflex changes in V_E and RSNA were measured in response to hypoxia. Tidal volume (V_t) and respiratory rate (RR) were calculated from the pressure changes in the chamber measured with a differential pressure transducer and amplifier (MP45, Validyne Engineering Corp., Northridge, CA, USA) connected to the PowerLab data acquisition system. Calibration of V_t was performed by varying the volume of the chamber with a calibrated plunger at 60 cycles min^{-1}. V_t was calculated from an adaptation of the formula of Drorbaugh and Fenn as described previously (Sun *et al.* 1999*b*). Ventilatory responses to hypoxia and hypercapnia were determined longitudinally in the same animal through the course of the study (before and after CHF induction, and after virus surgery).

RSNA responses to hypoxia were measured along with ventilation in these groups, 3 days after renal electrode implant concomitant with virus surgery. RSNA was recorded using a Grass P511 differential amplifier (Grass Technologies/Astro-Med Inc., West Warwick, RI, USA) and a storage oscilloscope. RSNA was filtered at a bandwidth of 100 Hz to 3 kHz, and the nerve signal was fed to an audio amplifier and loudspeaker. The RSNA signal was rectified and integrated, and both raw and integrated signals were recorded. All analog signals were captured and digitized by using a PowerLab (Model 8SP) data acquisition system.

Responses to chemoreceptor stimulation were measured in the conscious resting state. CB chemoreceptors were stimulated preferentially by allowing the rabbits to breathe graded mixtures of hypoxic gas under poikilocapnic conditions. Different concentrations of O_2 with balance of N_2 were delivered into the chamber in the following sequence: 21% O_2 (normoxia), 15% O_2 (mild hypoxia) and 10% O_2 (moderate hypoxia). Each stimulation was held for 2.5 min until a steady response was achieved. Ten minutes of recovery time at 21% O_2 was allowed between stimuli to ensure that all variables returned to baseline levels.

Apnoea/hypopnoea index and respiratory rate variability

Resting breathing pattern was determined by plethysmography and quantified as previously described (Marcus *et al.* 2014). To quantify respiratory disturbances associated with oscillatory breathing behaviour we calculated an apnoea/hypopnoea index (AHI), and a respiratory rate variability index (RRVI). The AHI was the total number of apnoeas and hypopnoeas occurring per hour. An apnoea or hypopnoea was counted if there was a 50% or greater reduction in V_t for three or more respiratory cycles. Post-sigh apnoeas were excluded from the analysis. Oscillations in respiratory rate (RRVI) were counted when there was a change in ventilatory rate greater than 3 standard deviations from the mean (taken over the course of 1 h). All events for AHI or RRVI were identified visually, counted and expressed as the number of events per hour (AHI) or the number of oscillations per hour (RRVI).

Arrhythmia incidence

Arrhythmia incidence was determined during the resting baseline periods from the ECG. Premature beats or delayed beats (beat to beat R–R interval greater than 3 standard deviations from the mean) or beats with ectopic foci were visually identified and recorded to determine an index of events per hour. All events meeting the stated criteria were counted and combined to derive a single index as previously described (Marcus *et al.* 2014).

Evaluation of heart rate variability

Heart rate variability (HRV) was derived from dP/dt blood pressure signal recorded at 10 kHz sampling rate from the radiotelemetry transmitter (Data Science International), and calculated on a beat-to-beat basis by using the Powerlab system and LabChart software (ADInstruments, Colorado Springs, CO, USA). HRV was analysed by using the HRV extension for LabChart 7 as previously described (Pliquett *et al.* 2003; Marcus *et al.* 2014). Briefly, beat-to-beat intervals were transformed by a fast Fourier transformation algorithm followed by Hann windowing at 256 points with 50% overlap. HRV in the time domain was analysed for the standard deviation of interpulse intervals (SDNN). Power spectral analysis in the frequency domain was performed using the following frequency cutoffs: 0.0625–0.1875 Hz was considered as the low-frequency (LF) band, and 0.1875–0.5625 Hz as the high-frequency (HF) band (Moguilevski *et al.* 1995). Total power integrated the whole spectrum.

Method of killing

At the conclusion of the experimental protocol all rabbits were humanely killed. In accordance with standards set out by the American Veterinary Medical Association and the Institutional Animal Care and Use Committee at University of Nebraska Medical Centre, all rabbits were killed with an intravenous overdose of pentobarbital (150 mg kg^{-1}) or Fatal Plus Euthanasia Solution (120 mg kg^{-1} for the first 4.5 kg of body weight and then 60 mg kg^{-1} for every 4.5 kg of body weight thereafter).

Immunofluorescence detection of KLF2 in the CB

After the animal had been killed, common carotid arteries were immediately perfused with ice-cold PBS (pH 7.4) for 10 min, followed by buffered paraformaldehyde (4%, Sigma, St Louis, MO, USA) for 10 min. The carotid artery bifurcations including the CBs were harvested from the rabbits and post-fixed by immersion in buffered paraformaldehyde 4% for 24–48 h at 4°C followed by three 15 min washes in PBS, sucrose gradient (5,10 and 20% in PBS), and then embedded in optimal cutting temperature medium. Cryostat sections (20 μm) of the CB were obtained and mounted on Superfrost Plus slides (Thermo Fisher Scientific Inc., Waltham, MA, USA). Sections were blocked/permeabilized in 0.5% Triton X-100, 2% fish skin gelatin (Sigma-Aldrich), 1% bovine serum albumin in PBS for 1 h at room temperature. Sections were incubated overnight at room temperature with a mixture of a goat anti-KLF2 polyclonal antibody (1:100 in the same blocking media, catalogue no. TA807009, OriGene, Rockville, MD, USA) and a mouse anti-tyrosine hydroxylase monoclonal antibody (1:250 in the same blocking media, catalogue no. MAB318, Millipore, Billerica, MA, USA), the latter used as a positive control for recognition of CB chemoreceptor cells. After being washed with PBS, tissue sections were incubated for 1 h with a mixture of Alexa-Fluor 546 rabbit anti goat IgG (1:200, Molecular Probes, Carlsbad, CA, USA) and Alexa-Fluor 647 rabbit anti-mouse IgG (1:200, Molecular Probes). Finally, sections were mounted in DAPI (4′,6-diamidino-2-phenylindole)-containing media (Vectashield, Vector Laboratory, Inc., Burlingame, CA, USA) and visualized using a confocal laser microscope (Leica, Wetzlar, Germany). A negative control was performed by omission of the primary antibody.

Western blot analysis of CB tissue

CB tissue was removed rapidly after death of the animal and immediately frozen on dry ice and subsequently stored at −80°C until analysis. Tissues were homogenized in RIPA buffer (50 mM Tris HCl pH 7.4, 150 mM NaCl, 2 mM EDTA, 1% NP-40, 0.1% SDS) and total protein was extracted from the homogenates. The concentration of protein extracted was measured using a protein assay kit (Pierce, Rockford, IL, USA) and samples were adjusted to the same concentration of protein with equal volumes of 2× 4% SDS sample buffer. The samples were boiled for 5 min followed by loading on a 7.5% SDS-PAGE gel (30 μg protein/10 μL per well) for electrophoresis using a Bio-Rad mini gel apparatus at 40 mA per gel for 45 min. The fractionated protein on the gel was transferred onto a PVDF membrane (Millipore) and electrophoresed at 300 mA for 90 min. The membrane was probed with KLF2 primary antibodies (KLF2 mouse polyclonal IgG, catalogue no. H00010365-A01, Novus Biologicals, Littleton, CO, USA, 1:1000) and secondary antibody (goat anti-mouse IgG HRP, no. 31430, ThermoFisher, 1:5000), and then treated with enhanced chemiluminescence substrate (Pierce) for 5 min at room temperature. The bands in the membrane were visualized and analysed using UVP Bioimaging Systems. After obtaining the KLF2 (45 kDa) blot density, the membrane was then treated using Restore Western Blot Stripping Buffer (Thermo Scientific) to remove the KLF2 signal, followed by probing with primary antibodies for β-tubulin (β-tubulin mouse monoclonal IgG, Abcam 8226, Abcam Biotechnology Inc., Cambridge, MA, USA, 1:5000) using the same process as the KLF2 antibodies to get the β-tubulin blot densities. An additional group of samples was used to determine CB expression of endothelial nitric oxide synthase (eNOS) and angiotensin-converting enzyme 1 (ACE1). The same methodology was used as described above for KLF2 with the substitution of the appropriate primary antibodies (eNOS mouse monoclonal IgG1, catalogue no. ab76198, Abcam, 1:1000; ACE1 mouse monoclonal IgG1, catalogue no. ab11734, Abcam, 1:100). The final reported data are the KLF2, eNOS or ACE1 band density normalized to β-tubulin.

Antibody specificity

All antibodies were procured from commercial sources (Abcam, Origene, Novus) that produce and verify their antibodies in-house. We further tested the specificity of the Novus KLF2 and Abcam eNOS and ACE1 antibodies using commercially produced HEK293 cell lysates transfected with a DDK-tagged empty vector or a DDK-tagged vector encoding KLF2 (Novus, NBL1-12319), eNOS (Novus, NBP2-10685) or ACE1 (Origene, LY433435). Equal protein loading was assessed using a Ponceau S stain. For KLF2, eNOS and ACE1, overexpression lysates showed distinct bands at an appropriate molecular weight while no bands were detected in the empty cell lysates (data not shown).

Data analysis

All parameters were recorded with a Powerlab data acquisition and analysis system. Integrated RSNA was expressed as the per cent of the maximal nerve activity evoked by eliciting the oropharyngeal reflex with a puff of cigarette smoke as previously described (Sun *et al.* 1999*b*, Li *et al.* 2006, Ding *et al.* 2011). Resting and chemoreflex-evoked respiratory responses (minute ventilation, V_E) were calculated as the product of tidal volume (V_t) and RR ($V_E = V_t \times$ RR) and expressed relative to body weight. Chemoreflex function curves were analysed by plotting data points averaged over 10 s for RSNA and V_E against the corresponding F_{IO_2}.

In paced rabbits, renal nerve electrodes were implanted after the development of CHF concomitant with virus delivery, and RSNA measurements were made 3 days after surgery. In rabbits that did not undergo pacing (scrambled siRNA or KLF2 siRNA), RSNA electrodes were implanted 3 weeks after transfection. This time interval of KLF2 knockdown mimicked the duration of time in which changes in blood flow and KLF2 expression would be affected in paced rabbits. The differences in resting and chemoreflex-evoked RSNA between groups as well as CB protein expression were determined using one-way ANOVA. Other variables were measured longitudinally through the course of pacing and virus delivery. Thus, chemoreflex V_E responses, measures of resting breathing pattern, ECG parameters and arrhythmia incidence in the experimental groups were analysed by a two-way repeated-measures ANOVA. The Sidak–Holm procedure was used to determine significance for pairwise comparisons of interest. All data are expressed as mean ± SEM. Statistical significance was accepted at $P < 0.05$.

Results

Effect of CHF and viral gene transfer on CB KLF2 expression

Immunofluorescence images as well as representative immunoblots of CB KLF2 protein expression are shown in Fig. 2. Qualitatively, the immunofluorescence images show that KLF2 expression in CB glomus cells was reduced in CHF-empty and with KLF2 siRNA, and that KLF2 expression was restored in CB tissue from CHF-KLF2 rabbits (Fig. 2*A*). Quantitatively, KLF2 protein expression (determined by western blot) was reduced by 50% in CB tissue from CHF rabbits receiving empty virus relative to sham (un-paced) rabbits (Fig. 2*B* and *C*). In CHF-KLF2

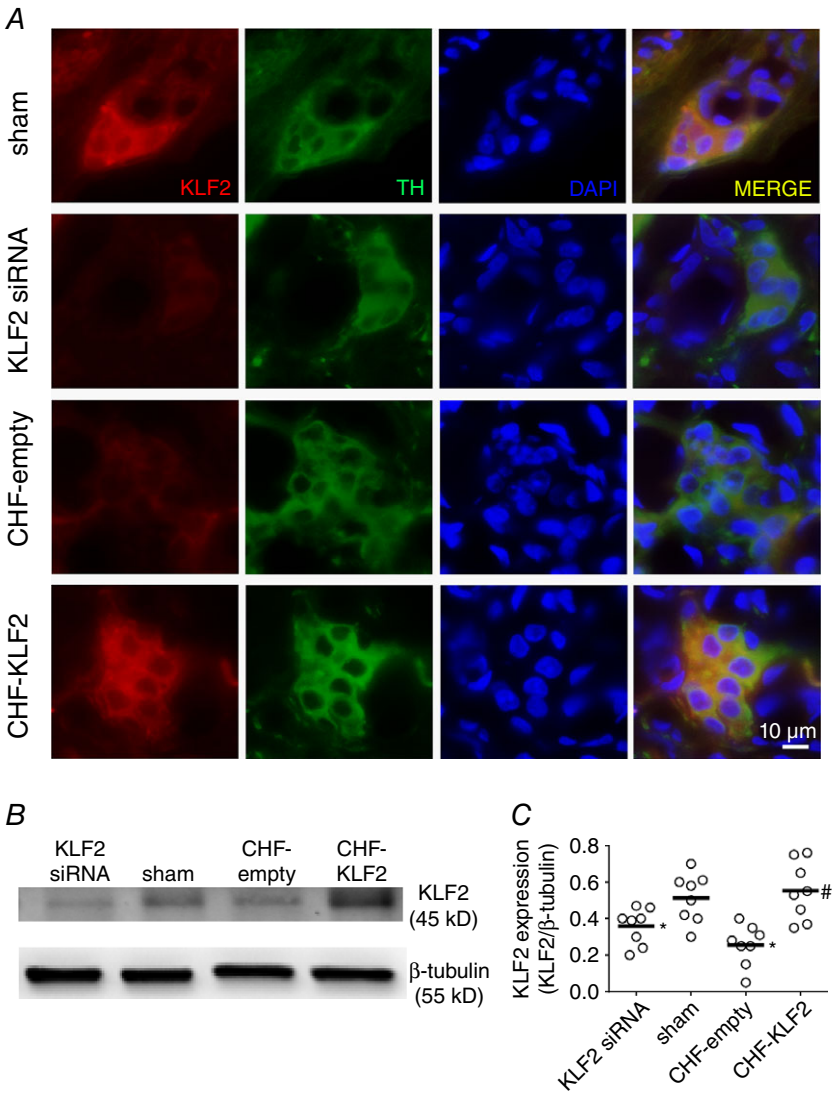

Figure 2. CB KLF2 protein expression is reduced in CHF rabbits
A, immunohistochemical images illustrating reduced KLF2 expression in glomus cells from CB of CHF and KLF2 siRNA rabbits, and enhanced KLF2 expression in glomus cells from CB of CHF-KLF2 rabbits. *B*, representative western blot showing that CB KLF2 expression is reduced in CHF and with siRNA knockdown, and that viral transfection with KLF2 restores CB KLF2 expression in CHF rabbits. *C*, mean data for CB KLF2 expression. For western blots, $n = 8$ rabbits per group. For immunohistochemistry, $n = 1$ per group. $^{*}P < 0.05$ *vs.* sham. $^{\#}P < 0.05$ *vs.* CHF-empty. Results are expressed as a scatter plot with mean indicated by the horizontal black bar.

Table 1. ECG measurements and body weight in CHF rabbits

Sham	Pre		Post
Body weight (kg)	3.6 ± 0.1		3.8 ± 0.2
LVd Vol (ml)	6.1 ± 0.7		6.8 ± 0.8
LVs Vol (ml)	2.3 ± 0.4		2.3 ± 0.3
Ejection fraction	63.0 ± 2.5		65.2 ± 2.0
Fractional shortening	32.5 ± 1.0		34.3 ± 1.8
CHF-empty	**Pre-pace**	**CHF**	**Post-virus**
Body weight (kg)	3.6 ± 0.1	3.6 ± 0.1	3.5 ± 0.2
LVd Vol (ml)	6.3 ± 0.5	7.0 ± 0.5	8.2 ± 0.5
LVs Vol (ml)	2.1 ± 0.2	3.9 ± 0.3*	4.9 ± 0.4*
Ejection fraction	66.7 ± 1.4	42.7 ± 2.6*	41.6 ± 2.2*
Fractional shortening	34.0 ± 1.0	19.9 ± 1.5*	18.7 ± 1.1*
CHF-KLF2	**Pre-pace**	**CHF**	**Post-virus**
Body weight (kg)	3.8 ± 0.1	3.9 ± 0.1	3.7 ± 0.2
LVd Vol (ml)	6.2 ± 0.5	8.5 ± 0.6	8.0 ± 0.6
LVs Vol (ml)	2.1 ± 0.2	5.2 ± 0.4*	4.8 ± 0.4*
Ejection fraction	66.6 ± 1.3	38.9 ± 1.1*	39.6 ± 1.2*
Fractional shortening	34.3 ± 1.0	17.3 ± 0.6*	17.6 ± 0.6*

LVd Vol = left ventricular diastolic volume; LVs Vol = left ventricular systolic volume, $n = 8$ rabbits per group. *$P < 0.05$ compared to pre-pace.

rabbits, CB KLF2 expression was significantly greater than in CHF-empty rabbits (Fig. 2*B* and *C*). In KLF2 siRNA rabbits, CB KLF2 expression was reduced relative to scrambled siRNA rabbits (0.35 ± 0.04 KLF2 siRNA *vs.* 0.50 ± 0.07 scrambled siRNA, $P < 0.05$).

Effect of CB KLF2 on cardiac function in CHF

After 3–4 weeks of pacing and in the resting state with the pacer turned off, ejection fraction and fractional shortening were reduced from pre-pace levels by ∼ 42% and 44% respectively, concomitant with increased left ventricular systolic (LVs Vol) dimensions in both CHF-empty and CHF-KLF2 groups (Table 1). Previous studies using the same model demonstrate that cardiac function is not altered through the course of the study in non-paced rabbits (Li *et al.* 2005, Ding *et al.* 2009, Marcus *et al.* 2014). In the CHF groups (CHF-empty and CHF-KLF2), the pacemaker was turned off for 24 h during the virus surgery and recovery and then reinstated. At 3 days following delivery of the empty virus (CHF-empty), ejection fraction and fractional shortening were not significantly different from the measurements in the same rabbits 1 day prior to empty virus surgery (Table 1). Similarly, ventricular volumes (LVd Vol and LVs Vol) after empty virus surgery were not significantly different from the measurement prior to surgery. In CHF-KLF2 rabbits no significant improvements in ejection fraction, fractional shortening, LVs Vol or LVd Vol were observed compared to the pre-KLF2 virus time point.

Effect of CB KLF2 on chemoreflex sensitivity in CHF

Changes in the sensitivity of the CBC with pacing (CHF) and the effect of CB KLF2 transfection are illustrated in Fig. 3. Activation of RSNA in response to hypoxia (F_{IO_2} 0.10) was markedly and significantly enhanced in CHF-empty rabbits compared to sham (+15 ± 2 Δ% max *vs.*+30 ± 8 Δ% max, $P < 0.05$ sham *vs.* CHF-empty respectively) but was attenuated in CHF-KLF2 rabbits (+23 ± 1 Δ% max, $P < 0.05$ *vs.* CHF-empty). Similarly, the hypoxic minute ventilatory (V_E) response (F_{IO_2} 0.10) was significantly enhanced in CHF-empty rabbits compared to sham (+125 ± 31 *vs.* +263 ± 24 Δml min kg^{-1}, respectively) and was also attenuated in CHF-KLF2 (+157 ± 32 Δml min kg^{-1}, $P < 0.05$ *vs.* CHF-empty).

To more definitively determine the role of KLF2 in chemoreflex function, and its contribution to autonomic dysfunction and breathing abnormalities, we performed an additional series of experiments in which we transfected the CB with KLF2 siRNA to selectively knock-down KLF2 in this tissue. Of primary interest, we observed that knockdown of KLF2 in the CB using siRNA in non-paced rabbits increased both the RSNA (+21 ± 2 Δ% max KLF2 siRNA) and V_E (+160 ± 29 Δml min^{-1} KLF2 siRNA) responses to hypoxia (F_{IO_2} 0.10) relative to non-paced rabbits which received CB transfection of a scrambled siRNA (+12 ± 2 Δ% max and +101 ± 22 Δml min^{-1}, RSNA and V_E respectively, $P < 0.05$). The V_E and RSNA responses to hypoxia in the scrambled siRNA group were similar to the hypoxic responses observed in sham rabbits without virus surgery (Fig. 3). Thus, reduction in CB KLF2 alone was sufficient to increase CBC sensitivity.

Ventilation under normoxia (F_{IO_2} 21%, F_{ICO_2} 0.03%) mild hypercapnia (F_{IO_2} 21%, F_{ICO_2} 5%) and moderate hypercapnia (F_{IO_2} 21%, F_{ICO_2} 7%) was measured in the plethysmograph to determine the chemoreflex sensitivity to hypercapnia. Using linear regression, the slope of the line defined by these points (F_{ICO_2} 0.03%, 5% and 7%) was determined and used as an index of the CO_2 sensitivity of the chemoreflex (HCVR, ml min^{-1} %CO_2 kg^{-1}). No statistically significant differences were observed between groups (sham 16.3 ± 2.8, CHF-empty 25.6 ± 3.4, CHF-KLF2 16.5 ± 2.0, scrambled siRNA 19.64 ± 2.7, KLF2 siRNA 24.3 ± 4.3, ANOVA $P = 0.1339$).

Effect of CB KLF2 on resting RSNA and oscillatory breathing in CHF

Resting RSNA in CHF-empty rabbits was nearly double that of the sham group (Fig. 3*A* and *B*). RSNA was significantly lower in CHF-KLF2 rabbits than in

CHF-empty rabbits (Fig. 3*A* and *B*) with a resting RSNA level like that of sham rabbits. Although arterial pressure tended to be lower with the development of CHF in both CHF-empty and CHF-KLF2 groups, no statistically significant differences were observed among sham, CHF-empty or CHF-KLF2 groups (Table 3). Importantly, we found that resting RSNA in non-paced rabbits that received CB KLF2 siRNA was significantly higher than in non-paced rabbits that received CB scrambled siRNA (Fig. 3*A* and *B*). Resting blood pressure was similar between groups while resting heart rate was significantly elevated in the CB KLF2 siRNA group (Table 3). Resting V_E was not different among sham and paced groups prior to initiation of the pacing protocol. In both CHF-empty and CHF-KLF2 groups there was a trend for V_E to increase from the pre-pace time point to the time point after CHF development just prior to virus surgery, although the differences were not statistically significant.

Oscillatory breathing patterns were observed in CHF-empty and CHF-KLF2 rabbits prior to virus surgery (Fig. 4*A*). Oscillations in respiratory rate and tidal volume were quantified with two different indexes, the AHI and RRVI. In CHF-empty rabbits, the AHI was significantly increased with the development of CHF at 3–4 weeks pacing compared to pre-pace, and continued to increase after delivery of the empty virus to the CB (Fig. 4*B*). In the CHF-KLF2 group, AHI increased to a similar extent in CHF but was significantly reduced after virus delivery (Fig. 4*B*). A similar pattern was observed in respiratory rate variability. In CHF-empty rabbits, the RRVI increased with the development of CHF and remained elevated after delivery of the empty virus to the CB, whereas in the CHF-KLF2 rabbits, the RRVI increased with CHF and was reduced after delivery of KLF2 to the CB in CHF (Fig. 4*B*). We also observed distinct phenotypic changes in respiratory patterns in the CB KLF2 siRNA group. In these rabbits, we observed oscillatory breathing patterns similar in nature to those observed in CHF-empty rabbits (Fig. 4*A*). Both AHI and RRVI were significantly higher in rabbits receiving CB KLF2 siRNA compared to rabbits receiving CB scrambled siRNA (Fig. 4*B*).

Effect of CB KLF2 on cardiac autonomic balance in CHF

All parameters of HRV analysis are included in Table 2. Time domain analysis revealed that the SDNN was significantly decreased from the pre-pace time point to the paced pre-virus time point (CHF) in CHF-empty and CHF-KLF2 groups, and CB KLF2 reversed this effect ($P < 0.05$). Delivery of the empty virus did not reverse decreases in SDNN. Using power spectral analysis, we determined that the total spectral power of HRV was

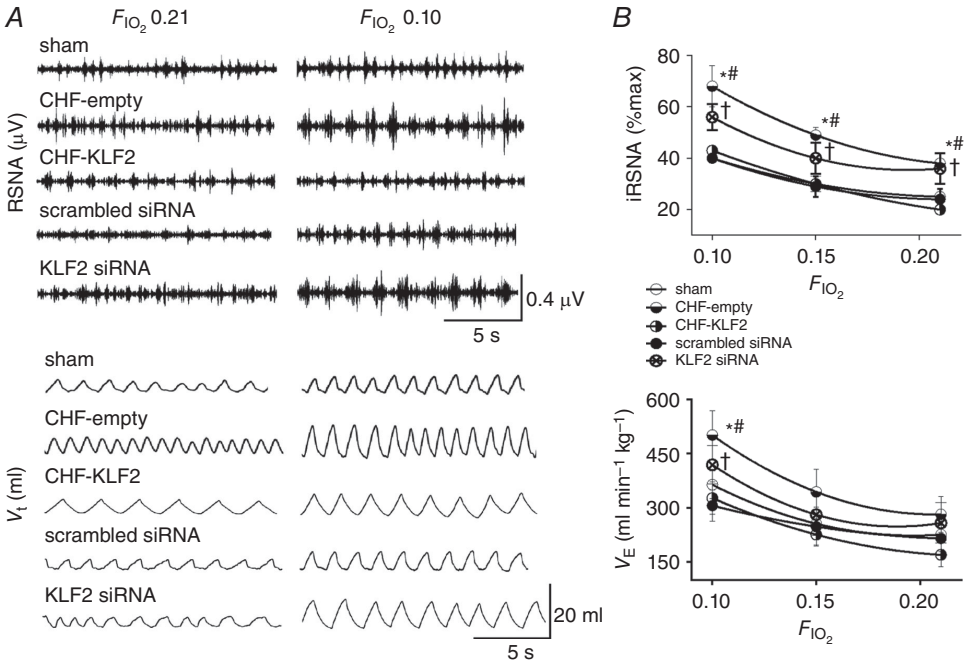

Figure 3. KLF2 mediates CB chemoreflex sensitivity and resting RSNA in CHF rabbits
A, representative records illustrating resting RSNA and ventilation and the response to poikilocapnic hypoxia (F_{IO_2} 0.10) in CHF rabbits with and without CB KLF2 transfection and in sham rabbits with CB KLF2 siRNA or CB scrambled siRNA. *B*, summary data showing enhanced resting RSNA and enhanced minute ventilation and RSNA responses to hypoxia in CHF-empty and KLF2 siRNA rabbits. CB KLF2 transfection had a salutary effect in CHF rabbits. $n = 8$ rabbits per group, except scrambled siRNA ($n = 6$). $^{*}P < 0.05$ CHF-empty *vs.* sham condition. $^{\#}P < 0.05$ CHF-empty *vs.* CHF-KLF2. Results are expressed as mean ± SEM.

significantly reduced from the pre-pace time point to the paced pre-virus time point (CHF) in CHF-empty and CHF-KLF2 groups, and CB KLF2 reversed this effect ($P < 0.05$). Delivery of the empty virus did not reverse decreases in total spectral power of HRV. The LF/HF ratio was increased from the pre-pace time point to the pre-virus time point (CHF) in CHF-empty and CHF-KLF2 groups. CB KLF2 had a salutary effect on LF/HF ratio ($P < 0.05$, Table 2), whereas no salutary effect was observed in the CHF-empty rabbits (Table 2). The increase in LF/HF ratio from the pre-pace time point to the pre-virus time point (CHF) was associated with a significant reduction in the HF component of HRV in CHF-empty and CHF-KLF2 rabbits. We observed no significant change in time domain measures of HRV (SDNN) in KLF2 siRNA rabbits, but spectral analysis of HRV indicated a significant increase in the ratio of low frequency to high frequency power of HRV (LF/HF) compared to pre-virus and scrambled siRNA rabbits. This change was characterized by significant increases in LF power and significant decreases in HF power. There was no significant difference between pre- and post-virus measurements of LF/HF in the scrambled siRNA group.

Effect of CB KLF2 on arrhythmia incidence in CHF

Because of the relationship between CBC sensitivity, sympathetic hyperactivity, disordered breathing and cardiac arrhythmias in CHF patients, we quantified arrhythmia incidence in our study. As shown in Fig. 5, there was a markedly higher incidence of arrhythmias at the paced pre-virus time point (CHF) in CHF-empty and CHF-KLF2 rabbits relative to the pre-pace time point or sham animals. After virus surgery, arrhythmia incidence remained elevated in CHF-empty rabbits, whereas in the CHF-KLF2 rabbits, arrhythmia incidence was significantly reduced (Fig. 5*C*). Arrhythmia incidence was not significantly different between sham, CB scrambled siRNA and CB KLF2 siRNA groups (Fig. 5*C*). Most arrhythmias we observed were premature ventricular contractions with a compensatory pause, but we also noted isolated sinus pauses as well as sustained bradyarrhythmias in one or two cases. CB KLF2 reduced arrhythmias with no selective effect on type.

Effect of CHF and viral gene transfer on CB eNOS and ACE1 expression

Representative immunoblots and quantification of CB ACE1 and CB eNOS are shown in Fig. 6. Analysis of CB tissue indicated that eNOS protein expression was significantly reduced in CB tissue from CHF rabbits receiving empty virus relative to sham (un-paced) rabbits. In CHF-KLF2 rabbits, expression of eNOS in CB tissue was similar to CHF-empty rabbits ($P = 0.33$). In KLF2 siRNA rabbits, CB eNOS expression was reduced

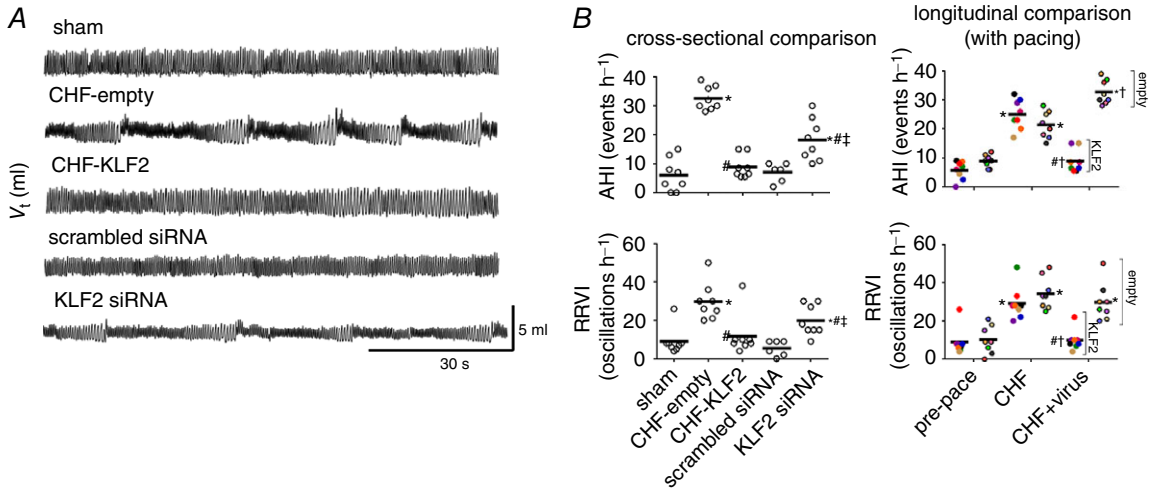

Figure 4. CB KLF2 contributes to oscillatory breathing in CHF rabbits
A, representative records of ventilation in CHF rabbits with KLF2 or empty virus transfection to the CB and in sham rabbits with CB KLF2 siRNA or CB scrambled siRNA transfection. Oscillatory breathing in CHF is virtually abolished by CB KLF2 transfection, whereas CB KLF2 siRNA transfection precipitates oscillatory breathing. *B*, mean data showing cross-sectional (left) and longitudinal (right) group comparisons of oscillatory breathing in CHF rabbits with CB KLF2 or CB empty transfection and sham rabbits transfected with KLF2 siRNA or scrambled siRNA as quantified by the apnoea hypopnea index (AHI) and respiratory rate variability index (RRVI). $n = 8$ rabbits per group, except scrambled siRNA ($n = 6$). $^{*}P < 0.05$ *vs.* pre-pace or sham. $^{\#}P < 0.05$ *vs.* CHF-empty. $^{\ddagger}P < 0.05$ *vs.* scrambled siRNA. $^{\dagger}P < 0.05$ *vs.* CHF. Results are illustrated as a scatter plot with mean indicated by the horizontal black bar. For longitudinal data, individual animals were assigned a specific colour, which may be observed at each respective timepoint.

Table 2. Heart rate variability analysis

Sham	Pre	Post
SDNN (ms)	14 ± 1	13 ± 1
Total power (ms^2)	200 ± 31	187 ± 37
LF (nu)	27 ± 5	25 ± 3
HF (nu)	47 ± 3	40 ± 2
LF/HF ratio	0.6 ± 0.1	0.6 ± 0.1
CHF-empty	**Pre-pace**	**CHF**	**CHF post-virus**
SDNN (ms)	14 ± 1	9 ± 1*	8 ± 1*#
Total power (ms^2)	192 ± 30	66 ± 14*	70 ± 22*#
LF (nu)	22 ± 4	25 ± 3	30 ± 5
HF (nu)	36 ± 5	25 ± 3	26 ± 4#
LF/HF ratio	0.6 ± 0.1	1.0 ± 0.1*	1.2 ± 0.2*#
CHF-KLF2	**Pre-pace**	**CHF**	**CHF post-virus**
SDNN (ms)	15 ± 1	10 ± 1*	15 ± 2†
Total power (ms^2)	196 ± 47	91 ± 15*	210 ± 49†
LF (nu)	19 ± 3	23 ± 4	22 ± 3
HF (nu)	39 ± 3	27 ± 2*	43 ± 4†
LF/HF ratio	0.5 ± 0.1	0.8 ± 0.1*	0.5 ± 0.1†
Scrambled siRNA	**Pre-virus**	**Post-virus**
SDNN (ms)	14 ± 3	15 ± 4
Total power (ms^2)	185 ± 78	233 ± 125
LF (nu)	31 ± 3	25 ± 3
HF (nu)	49 ± 3	39 ± 3
LF/HF ratio	0.7 ± 0.1	0.7 ± 0.1
KLF2 siRNA	**Pre-virus**	**Post-virus**
SDNN (ms)	14 ± 2	12 ± 1
Total power (ms^2)	194 ± 38	159 ± 25
LF (nu)	19 ± 3	29 ± 3*
HF (nu)	46 ± 3	35 ± 3*
LF/HF ratio	0.4 ± 0.1	0.9 ± 0.2*

SDNN = standard deviation of the normalized RR interval; LF = low-frequency power; HF = high-frequency power; nu = normalized units. *$P < 0.05$ compared to respective baseline condition (pre-pace or pre-virus), #$P < 0.05$ compared to sham, †$P < 0.05$ compared to CHF. $n = 8$ rabbits per group, except scrambled siRNA ($n = 6$).

Table 3. Baseline cardiovascular variables

Sham	Pre	Post
MAP (mmHg)	66 ± 2	70 ± 8
HR (bpm)	200 ± 13	201 ± 9
CHF-empty	**Pre-pace**	**CHF**	**CHF post-virus**
MAP (mmHg)	71 ± 5	62 ± 5	62 ± 9
HR (bpm)	205 ± 6	222 ± 4*	224 ± 8*
CHF-KLF2	**Pre-pace**	**CHF**	**CHF post-virus**
MAP (mmHg)	78 ± 5	66 ± 7	62 ± 8*
HR (bpm)	209 ± 7	225 ± 11	193 ± 5*†
Scrambled siRNA	**Pre-virus**	**Post-virus**
MAP (mmHg)	76 ± 7	68 ± 10
HR (bpm)	204 ± 5	198 ± 11
KLF2 siRNA	**Pre-virus**	**Post-virus**
MAP (mmHg)	74 ± 7	82 ± 6
HR (bpm)	203 ± 6	210 ± 6

MAP = mean arterial pressure, HR = heart rate. $n = 8$ rabbits per group, except scrambled siRNA ($n = 6$). *$P <$ 0.05 compared to respective baseline condition (pre-pace or pre-virus), †$P < 0.05$ compared to CHF, #$P < 0.05$ compared to CHF-empty.

relative to sham rabbits. Conversely, ACE1 protein expression was significantly increased in CB tissue from CHF rabbits receiving empty virus relative to sham (un-paced) rabbits. In KLF2 siRNA rabbits, CB ACE1 expression was significantly increased relative to sham rabbits.

Discussion

Our results confirm a role for KLF2 in the enhanced CBC function observed in experimental CHF. We show that restoration of CB KLF2 and subsequent reduction in CBC sensitivity is sufficient to improve autonomic imbalance, abnormal oscillatory breathing patterns and arrhythmia incidence associated with CHF. Viral transfection of the CB with KLF2 was an effective means of reducing both tonic and hypoxia-evoked RSNA in CHF, as well as improving HRV measures of cardiac sympatho-vagal balance. Furthermore, CB KLF2 attenuated ventilatory responses to hypoxia and decreased all indices of oscillatory breathing. These results lend further support to the hypothesis that enhanced CBC sensitivity plays an important role in the occurrence of autonomic dysfunction and disordered breathing patterns in CHF. In support of this notion, we show for the first time that knockdown of CB KLF2 in healthy rabbits is sufficient to enhance CBC sensitivity and recapitulate the autonomic and breathing instability associated with enhanced CBC sensitivity in CHF. Cumulatively, these results support the notion that reductions in CB KLF2 contribute importantly to enhanced CBC sensitivity and the resulting cardiac, autonomic, respiratory and haemodynamic maladaptations associated with CHF.

Carotid body blood flow and chemoreflex sensitivity

A significant body of work indicates that enhanced CB chemoreceptor activity in CHF is mediated by decreased bioavailability of neuro-inhibitory gasotransmitters

(Li *et al.* 2006; Ding *et al.* 2008; Schultz *et al.* 2012), increased production of neuro-excitatory hormones (Li *et al.* 2006) and a pro-oxidative shift in redox balance (Li *et al.* 2007; Ding *et al.* 2009, 2011). In addition to these biochemical changes, we have previously shown that CHF is associated with persistent reductions in CB blood flow that precede the development of enhanced CBC sensitivity (Ding *et al.* 2011), and that CB blood flow reduction per se (in the absence of CHF) is sufficient to elicit biochemical changes and enhanced CB function like that observed in CHF. These findings suggest that a blood flow-dependent mechanism contributes to enhanced CBC sensitivity in CHF. KLF2 is induced by vascular shear stress and is down-regulated in low-flow states (Dekker *et al.* 2005; Parmar *et al.* 2006), thus providing a potential link between KLF2 and CBC sensitivity in CHF. Our findings confirm the hypothesized relationship between KLF2 and CBC sensitivity and underline its importance to cardio-respiratory control in CHF.

Potential mechanisms of KLF2-mediated improvement in CBC sensitivity in CHF

KLF2 is a suitable candidate gene for our hypothesis because it is sensitive to reductions in blood flow, but also because it controls transcription of several genes that are particularly relevant to CBC dysfunction. Induction of KLF2 has been shown to repress ACE1 expression and to induce eNOS and heme-oxygenase expression in endothelial cells (Parmar *et al.* 2006). In concordance with this, we have found that increases in CB KLF2 expression that accompany treatment with Simvastatin in CHF rats are associated with increased CB eNOS and decreased CB AT1R expression and are associated with decreased CBC sensitivity, abnormal breathing patterns and arrhythmia incidence (Haack *et al.* 2014). Our present data show that knock-down of CB KLF2 using a viral vector increased CB ACE1 and decreased CB eNOS expression in healthy rabbits (Fig. 6), resulting in increased CBC sensitivity and resting RSNA, and development of abnormal oscillatory breathing patterns. Furthermore, restoring CB KLF2 in CHF rabbits attenuated increases in CB ACE1 expression (Fig. 6) and attenuated increases in CBC sensitivity, resting RSNA, abnormal oscillatory breathing patterns and arrhythmia incidence. Together, these data indicate that decreased CB KLF2 in CHF leads to increases in ACE1 expression and decreases in eNOS expression, which in turn may contribute to a neuro-excitatory phenotype in the CB via increased angiotensin II levels and decreased NO bioavailability (Li *et al.* 2005, 2006, 2007).

Induction of KLF2 also has a powerful influence on cellular redox state as it controls expression of several mediators of antioxidant defence (Fledderus *et al.* 2008; Kawanami *et al.* 2009). Persistent reductions in CB KLF2 in CHF could result in upregulation of pro-oxidant systems (angiotensin II activation of NADPH oxidase) as well as downregulation of antioxidant defences. Further exacerbation of oxidative stress could occur due to intermittent hypoxia (Nanduri *et al.* 2009) during episodes of sleep disordered breathing, which is highly prevalent in patients with CHF (Vazir *et al.* 2007). The role of inflammation in CBC function in CHF has not been evaluated to date, but the possibility that KLF2 mediates CBC sensitivity in CHF by regulation of inflammatory pathways should be considered. Inflammation has been shown to play a role in enhanced CBC sensitivity in animal

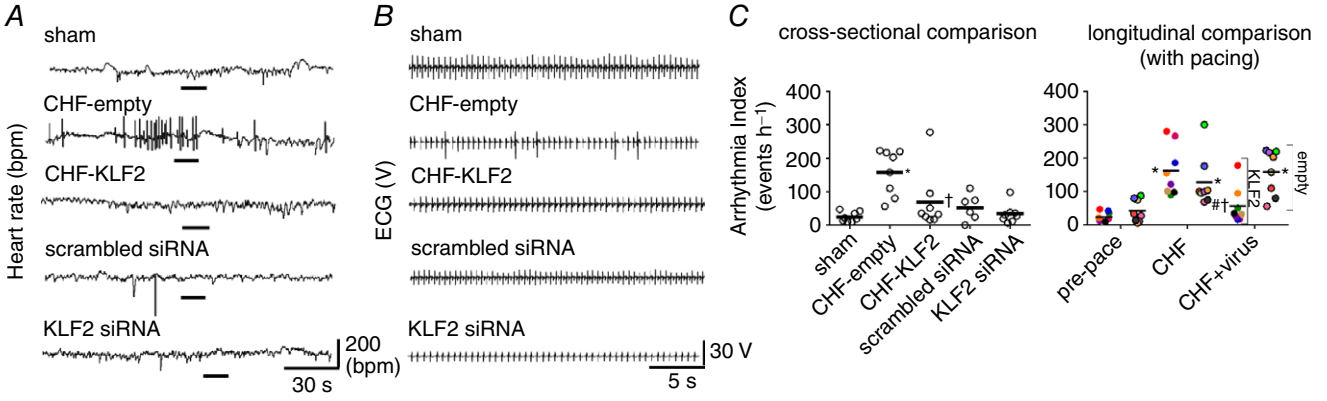

Figure 5. Effect of KLF2-mediated increases in CB chemoreflex sensitivity on arrhythmia incidence in CHF rabbits
A, representative tachograms illustrating increased arrhythmia incidence in CHF, and the salutary effect of CB KLF2 transfection. *B*, ECG traces taken during the period indicated by the black bar in *A*. *C*, cross-sectional and longitudinal summary data for the arrhythmia index. $n = 8$ rabbits per group, except scrambled siRNA ($n = 6$). $^{*}P < 0.05$ *vs.* pre-pace. $^{\#}P < 0.05$ *vs.* CHF (within group, longitudinal). $^{\dagger}P < 0.05$ *vs.* CHF-empty. Results are illustrated as a scatter plot with mean indicated by the horizontal black bar. For longitudinal data, individual animals were assigned a specific colour, which may be observed at each respective timepoint.

models of sleep apnoea (Del Rio *et al.* 2012; Iturriaga *et al.* 2015). KLF2 controls several genes that are involved in inflammation, and induction of KLF2 promotes an anti-inflammatory phenotype (Fledderus *et al.* 2008). Thus, restoration of CB KLF2 in CHF could improve CBC function by reducing inflammation and oxidative stress.

Our results indicate that CB KLF2 reduces enhanced CBC sensitivity in CHF, and we propose that this is probably related to multiple interrelated KLF2-dependent mechanisms (increased NOS and heme-oxygenase expression, decreased renin–angiotensin system activity, decreased oxidative stress and decreased inflammation). The improvement in CBC sensitivity normalized disordered breathing patterns, improved autonomic dysregulation and decreased the incidence of cardiac arrhythmias which are common in the CHF state.

Limitations

The hypoxia exposures used to test the CBC in our study are poikilocapnic in nature. Reductions in CO_2 associated with an enhanced HVR (as previously observed in CHF) would be expected to reduce the drive to breathe by driving down P_{aCO_2} and increasing pH. As such this would be expected to dampen the HVR over time in animals with an enhanced chemoreflex. We expect that this experimental design underestimates differences in HVR rather than overestimating them and that the enhanced HVR observed in CHF rabbits would probably be more robust if CO_2 were not allowed to fall. We feel that this point strengthens our conclusions, although we acknowledge that the data in this study are not a pure representation of the HVR because of presumed differences in P_{aCO_2} between groups and attendant effects on the drive to breathe.

The whole-body plethysmograph used to assess respiratory pattern and minute ventilation in these studies requires temporarily sealing the plexiglass box containing the animal to make an accurate assessment of tidal volume. We acknowledge that sealing the box has the potential to disturb the animal and cause it to alter its breathing pattern. It is important to note, however, that the rabbits used in this study were habituated to the plethysmograph and the procedure for chemoreflex testing before any experimental studies were conducted. Thus, while we acknowledge that this procedure may potentially alter respiratory pattern, we would like to emphasize that we have used habituation procedures intended to minimize behavioural responses to the plethysmograph, and any changes that do occur would be expected to affect all groups equally.

Clinical implications

Clinical studies indicate that disordered breathing patterns, autonomic dysregulation and increased arrhythmia incidence are highly prevalent in patients with CHF and are positively correlated with enhanced chemosensitivity (Giannoni *et al.* 2008). Of 60 CHF patients with sleep disordered breathing in this study, 13% had enhanced hypoxic and 12% had enhanced hypercapnic ventilatory responses in isolation while 27% had combined enhanced hypoxic and hypercapnic ventilatory responses (Giannoni *et al.* 2008). In our more controlled animal model of CHF in rabbits, all animals in CHF demonstrated enhanced hypoxic ventilatory responses with only mild or minimal changes in hypercapnic responses. A recent paper (Peng *et al.* 2017) has shown that in a mouse model of sleep apnoea, the prevalence of sleep disordered breathing was higher in animals with enhanced hypoxic chemosensitivity and that the hypercapnic ventilatory response was not significantly enhanced in these animals. Taken together, the present study and these findings suggest that enhanced CB hypoxic sensitivity alone may be sufficient

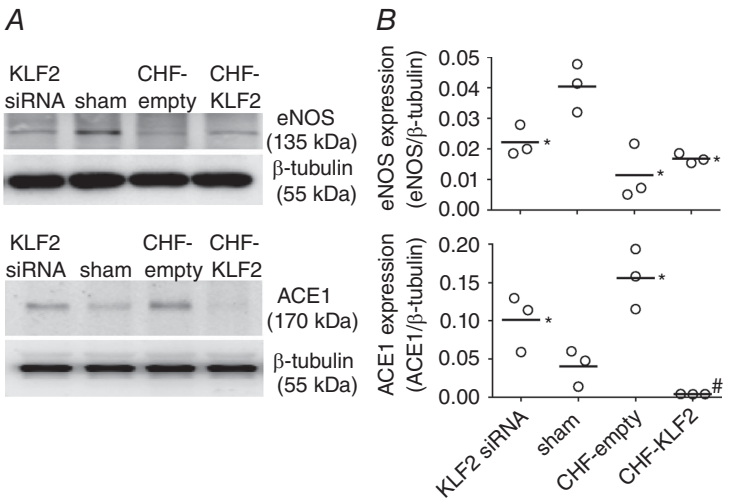

Figure 6. CB ACE1 and eNOS expression in CHF rabbits
Representative western blot (*A*) and mean data (*B*) showing that CB eNOS expression is reduced in CHF and with KLF2 siRNA knockdown, and that CB ACE1 expression is increased in CHF and reduced by viral transfection with KLF2. $^{*}P < 0.05$ *vs.* sham. $^{\#}P < 0.05$ *vs.* CHF-empty. $n = 3$ rabbits per group. Results are expressed as a scatter plot with mean indicated by the horizontal black bar.

to support abnormal respiratory patterns and autonomic dysregulation.

There has been increased interest in recent years in targeting CB chemoreceptor function as a means of improving autonomic dysregulation in cardiovascular diseases (Paton *et al.* 2013). We have published two studies in different CHF models confirming that bilateral CB ablation is indeed a viable means of improving autonomic and cardiac function, and reducing disordered breathing and mortality in CHF (Del Rio *et al.* 2013; Marcus *et al.* 2014). We have previously shown that CB KLF2 expression is reduced in CHF concomitant with enhanced CBC sensitivity, and that higher CB KLF2 in rats treated with Simvastatin is associated with reduced CBC sensitivity (Haack *et al.* 2014). Our current findings confirm the importance of this association and more directly demonstrate the importance of KLF2 to CBC function in CHF. Cumulatively, these results support the notion that reductions in CB KLF2 contribute importantly to enhanced CBC sensitivity, and that restoring its expression can effectively reduce the resulting cardiac, autonomic, respiratory and haemodynamic maladaptations associated with CHF without destroying the functionality of the CBC. Thus, novel therapeutic approaches which induce KLF2 may prove beneficial in the treatment of CHF.

Conclusions

Our results indicate that selective delivery of KLF2 to the CB reduces chemoreflex sensitivity, resting RSNA, disordered breathing and arrhythmia incidence, and improves cardiac autonomic function in a rapid-ventricular pacing model of CHF in rabbits. These findings suggest that KLF2 mediates increases in CBC sensitivity in CHF and therapeutic modalities that increase KLF2 in the CB may improve cardiac function by reducing sympathetic outflow and disordered breathing associated with CHF.

References

Dekker RJ, van Thienen JV, Rohlena J, de Jager SC, Elderkamp YW, Seppen J, de Vries CJ, Biessen EA, van Berkel TJ, Pannekoek H & Horrevoets AJ (2005). Endothelial KLF2 links local arterial shear stress levels to the expression of vascular tone-regulating genes. *Am J Pathol* **167**, 609–618.

Del Rio R, Moya EA & Iturriaga R (2012). Contribution of inflammation on carotid body chemosensory potentiation induced by intermittent hypoxia. *Adv Exp Med Biol* **758**, 199–205.

Del Rio R, Marcus NJ & Schultz HD (2013). Carotid chemoreceptor ablation improves survival in heart failure: rescuing autonomic control of cardiorespiratory function. *J Am Coll Cardiol* **62**, 2422–2430.

Ding Y, Li YL & Schultz HD (2008). Downregulation of carbon monoxide as well as nitric oxide contributes to peripheral chemoreflex hypersensitivity in heart failure rabbits. *J Appl Physiol* **105**, 14–23.

Ding Y, Li YL & Schultz HD (2011). Role of blood flow in carotid body chemoreflex function in heart failure. *J Physiol* **589**, 245–258.

Ding Y, Li YL, Zimmerman MC & Schultz HD (2010). Elevated mitochondrial superoxide contributes to enhanced chemoreflex in heart failure rabbits. *Am J Physiol Regul Integr Comp Physiol* **298**, R303–R311.

Ding Y, Li YL, Zimmerman MC, Davisson RL & Schultz HD (2009). Role of CuZn superoxide dismutase on carotid body function in heart failure rabbits. *Cardiovasc Res* **81**, 678–685.

Fledderus JO, Boon RA, Volger OL, Hurttila H, Ylä-Herttuala S, Pannekoek H, Levonen AL & Horrevoets AJ (2008). KLF2 primes the antioxidant transcription factor Nrf2 for activation in endothelial cells. *Arterioscler Thromb Vasc Biol* **28**, 1339–1346.

Giannoni A, Emdin M, Poletti R, Bramanti F, Prontera C, Piepoli M & Passino C (2008). Clinical significance of chemosensitivity in chronic heart failure: influence on neurohormonal derangement, Cheyne-Stokes respiration, and arrhythmias. *Clin Sci (Lond)* **114**, 489–497.

Grundy D (2015). Principles and standards for reporting animal experiments in *The Journal of Physiology* and *Experimental Physiology*. *J Physiol* **593**, 2547–2549.

Houser SR, Margulies KB, Murphy AM, Spinale FG, Francis GS, Prabhu SD, Rockman HA, Kass DA, Molkentin JD, Sussman MA & Koch WJ (2012). Animal models of heart failure: a scientific statement from the American Heart Association. *Circ Res* **111**, 131–150.

Haack KK, Marcus NJ, Del Rio R, Zucker IH & Schultz HD (2014). Simvastatin treatment attenuates increased respiratory variability and apnoea/hypopnoea index in rats with chronic heart failure. *Hypertension* **63**, 1041–1049.

Iturriaga R, Moya EA & Del Rio R (2015). Inflammation and oxidative stress during intermittent hypoxia: the impact on chemoreception. *Exp Physiol* **100**, 149–155.

Kawanami D, Mahabeleshwar GH, Lin Z, Atkins GB, Hamik A, Haldar SM, Maemura K, Lamanna JC & Jain MK (2009). Kruppel-like factor 2 inhibits hypoxia-inducible factor 1α expression and function in the endothelium. *J Biol Chem* **284**, 20522–20530.

Li YL, Gao L, Zucker IH & Schultz HD (2007). NADPH oxidase-derived superoxide anion mediates angiotensin II-enhanced carotid body chemoreceptor sensitivity in heart failure rabbits. *Cardiovasc Res* **75**, 546–554.

Li YL, Li YF, Liu D, Cornish KG, Patel KP, Zucker IH, Channon KM & Schultz HD (2005). Gene transfer of neuronal nitric oxide synthase to carotid body reverses enhanced chemoreceptor function in heart failure rabbits. *Circ Res* **97**, 260–267.

Li YL, Xia XH, Zheng H, Gao L, Li YF, Liu D, Patel KP, Wang W, & Schultz HD (2006). Angiotensin II enhances carotid body chemoreflex control of sympathetic outflow in chronic heart failure rabbits. *Cardiovasc Res* **71**, 129–138.

Marcus NJ, Del Rio R, Schultz EP, Xia XH & Schultz HD (2014). Carotid body denervation improves autonomic and cardiac function and attenuates disordered breathing in congestive heart failure. *J Physiol* **592**, 391–408.

Moguilevski V, Oliver J & McGrath BP (1995). Sympathetic regulation in rabbits with heart failure: experience using power spectral analysis of heart rate variability. *Clin Exp Pharmacol Physiol* **22**, 475–477.

Nanduri J, Wang N, Yuan G, Khan SA, Souvannakitti D, Peng YJ, Kumar GK, Garcia JA & Prabhakar NR (2009). Intermittent hypoxia degrades HIF-2α via calpains resulting in oxidative stress: implications for recurrent apnoea-induced morbidities. *Proc Natl Acad Sci USA* **106**, 1199–1204.

Naughton MT, Benard DC, Liu PP, Rutherford R, Rankin F & Bradley TD (1995). Effects of nasal CPAP on sympathetic activity in patients with heart failure and central sleep apnoea. *Am J Respir Crit Care Med* **152**, 473–479.

Parmar KM, Larman HB, Dai G, Zhang Y, Wang ET, Moorthy SN, Kratz JR, Lin Z, Jain MK, Gimbrone MA Jr & García-Cardeña G (2006). Integration of flow-dependent endothelial phenotypes by Kruppel-like factor 2. *J Clin Invest* **116**, 49–58.

Paton JF, Sobotka PA, Fudim M, Engleman ZJ, Hart EC, McBryde FD, Abdala AP, Marina N, Gourine AV, Lobo M, Patel N, Burchell A, Ratcliffe L & Nightingale A (2013). The carotid body as a therapeutic target for the treatment of sympathetically mediated diseases. *Hypertension* **61**, 5–13.

Peng YJ, Zhang X, Gridina A, Chupikova I, McCormick DL, Thomas RJ, Scammell TE, Kim G, Vasavda C, Nanduri J, Kumar GK, Semenza GL, Snyder SH, Prabhakar NR (2017). Complementary roles of gasotransmitters CO and H_2S in sleep apnea. *Proc Natl Acad Sci USA* **114**, 1413–1418.

Pliquett, RU, Cornish, KG & Zucker, IH (2003). Statin therapy restores sympathovagal balance in experimental heart failure. *J Appl Physiol* **95**, 700–704.

Ponikowski P, Chua TP, Anker SD, Francis DP, Doehner W, Banasiak W, Poole-Wilson PA, Piepoli MF & Coats AJ (2001). Peripheral chemoreceptor hypersensitivity: an ominous sign in patients with chronic heart failure. *Circulation* **104**, 544–549.

Schultz HD, Del Rio R, Ding Y & Marcus NJ (2012). Role of neurotransmitter gases in the control of the carotid body in heart failure. *Respir Physiol Neurobiol* **184**, 197–203.

Sun SY, Wang W, Zucker IH & Schultz HD (1999*a*). Enhanced activity of carotid body chemoreceptors in rabbits with heart failure: role of nitric oxide. *J Appl Physiol* **86**, 1273–1282.

Sun SY, Wang W, Zucker IH & Schultz HD (1999*b*). Enhanced peripheral chemoreflex function in conscious rabbits with pacing-induced heart failure. *J Appl Physiol* **86**, 1264–1272.

van de Borne P, Oren R, Abouassaly C, Anderson E & Somers VK (1998). Effect of Cheyne-Stokes respiration on muscle sympathetic nerve activity in severe congestive heart failure secondary to ischemic or idiopathic dilated cardiomyopathy. *Am J Cardiol* **81**, 432–436.

Vazir A, Hastings PC, Dayer M, McIntyre HF, Henein MY, Poole-Wilson PA, Cowie MR, Morrell MJ & Simonds AK. (2007). A high prevalence of sleep disordered breathing in men with mild symptomatic chronic heart failure due to left ventricular systolic dysfunction. *Eur J Heart Fail* **9**, 243–250.

Zucker IH, Schultz HD, Li YF, Wang Y, Wang W & Patel KP (2004). The origin of sympathetic outflow in heart failure: the roles of angiotensin II and nitric oxide. *Prog Biophys Mol Biol* **84**, 217–232.

Additional information

Competing interests

The authors declare no competing interests.

Author contributions

All experiments were performed in the Department of Cellular and Integrative Physiology at University of Nebraska Medical Center. H.D.S., N.J.M., R.D.R. and Y.D. contributed to the conception and design of the experiments. N.J.M. collected, analysed and interpreted data and drafted and revised the manuscript. R.D.R. contributed to analysis and interpretation of data, and drafting and revising of the manuscript. Y.D. contributed to the collection, analysis and interpretation of preliminary data. H.D.S. supervised the study, procured the resources to perform the study, and contributed to analysis and interpretation of data and manuscript revision. All authors approved the manuscript and agree to be accountable for all aspects of the work.

Funding

This study was funded by a Program Project Grant from the Heart, Lung, and Blood Institute of NIH (PO1-HL62222). N.J.M. was supported by a National Research Service Award fellowship from the Heart, Lung and Blood Institute of NIH (F32-HL108592-01A1).

Acknowledgements

The authors wish to thank Kaye Talbitzer for her surgical assistance, Dr Kurtis G. Cornish for management of the heart failure animal core at University of Nebraska Medical Center and Mary Ann Zink for her technical support.